Annals of the Academy of Romanian Scientists
Series on Physics and Chemistry
Online ISSN **2559 – 1061** Volume **10**, Number 2/**2025**

SURFACE TENSION EFFECTS ON THE FREE DROP DYNAMICS

Maria TOMOAIA-COTISEL[1,2], Gheorghe TOMOAIA[2,3], Aurora MOCANU[1*]

Abstract. *The effects of the surfactant adsorption on the surface of a free liquid drop, immersed in an unbounded liquid (the densities of the two bulk liquids are equal) are studied. The interfacial tension gradients, caused by the surfactant applied on the drop surface, generate surface forces within the boundary region of the free drop, leading to a surface flow (known as Marangoni flow). As a result of this flow, which causes the motion of neighboring liquids by viscous traction, a hydrodynamic pressure force (named Marangoni force) is generated which acts on the free drop surface. The aim of this research study is to correlate the effects of interfacial tension gradients, in a real surface flow, with the forces of hydrodynamic pressure, acting on the free drop surface. The Marangoni force is examined on nondeformable and deformable free drops. Dynamics of free liquid drops is known as the interfacial Marangoni effect. This effect has an important impact on surface flow of liquids in the absence of gravity, as well as in advanced fundamental research in physical chemistry, colloidal science, biological phenomena and in medical applications.*

Keywords: free drop dynamics, interfacial tension gradient, Marangoni force, Marangoni effect, Marangoni flow, hydrodynamic model

DOI [10.56082/annalsarsciphyschem.2025.2.15](https://doi.org/10.56082/annalsarsciphyschem.2025.2.15)

1. Introduction

The boundary between two immiscible liquid phases is known as the interfacial zone or, the interface. It is the thin layer surrounding a geometric surface of separation, in which the physical properties differ much from those in either of the bulk phases. The thickness of this layer is imprecise because the variations of physical properties across it are continuous. We shall consider it as infinitely thin, i.e., as a geometric surface. Since the thickness of interface is of the order of

[1] Professor, Dr. Babes-Bolyai University of Cluj-Napoca, Faculty of Chemistry and Chemical Engineering, Scientific Research Centre of Excellence in Physical Chemistry, 11 Arany Janos St., RO-400028, Cluj-Napoca, Romania; mcotisel@gmail.com
[2] Academy of Romanian Scientists, 3 Ilfov St., RO-050044, Bucharest, Romania
[3] Emeritus Professor Dr., Habil., MD Iuliu Hatieganu University of Medicine and Pharmacy, Department of Orthopedics and Traumatology, 47 General Traian Mosoiu St., RO-400132, Cluj-Napoca, Romania; tomoaia2000@yahoo.com
[4] Associated Professor Dr. Babes-Bolyai University of Cluj-Napoca, Faculty of Chemistry and Chemical Engineering, Scientific Research Centre of Excellence in Physical Chemistry, 11 Arany Janos St., RO-400028, Cluj-Napoca, Romania
* Corresponding author: mocanu.aurora@gmail.com

molecular dimensions, such an approximation is justified in treating the macroscopic movements of liquids.
Previously, we have explored the various movements of free drops, generated by the forces of hydrodynamic pressure, when the drop surface was covered by a surfactant, primarily based on the original research work directed by *Eminent Professor* **Emil Chifu** *et al.* [1-7] at Babes-Bolyai University of Cluj-Napoca, ***UBB,*** Faculty of Chemistry and Chemical Engineering, ***FCIC***. It is important to emphasize that some research studies are part of the ***first international research project*** of **UBB** and the National Aeronautics and Space Administration, **NASA**, of the United States of America, through National Council for Science and Technology, **CNST**, in Romania (1977-1987), gained by Professor Emil Chifu on "Surface flow of liquids in the absence of gravity", [1], through *an international scientific research competition*.

Therefore, the goal of this research work is to present some advanced theoretical models and experiments further developed by the academic research group, established by Professor **Emil Chifu**, in the physical chemistry laboratories at FCIC, UBB, which became the Scientific Research Center of Excellence in Physical Chemistry, **CECHIF,** founded in 2006, under the leadership of the director Professor Maria Tomoaia-Cotisel (2006-present) to deeply investigate the free drop dynamics and related interfacial phenomena.

To explain the free drop dynamics, it was suggested that Marangoni instability and capillary forces are important factors in drop movements and deformations [2,3]. To assess which one from these is a major factor on the drop dynamics, in this work, we investigate experimentally and theoretically the effect of local changes in the surface tension, σ, which are induced by the adsorption of a surfactant on the drop surface.

As a result of the adsorption of a surfactant (also called surface active compound), a surface tension gradient (Marangoni effect) appears, which generates a real surface flow, from low to high surface tension, called the *Marangoni flow*, and it is illustrated in Figure 1. This Marangoni interfacial flow causes the motion of the neighboring liquids by viscous traction [3-6], and generates the force of hydrodynamic pressure, named *Marangoni force*, which acts on the free drop surface.

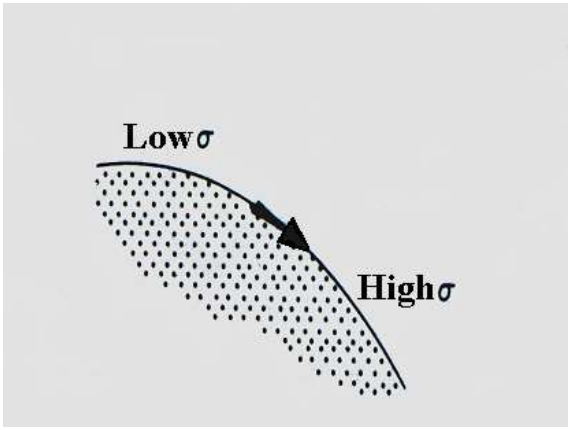

Fig. 1. Marangoni interfacial flow resulting under a surface tension, σ, gradient.

We have also developed a *theoretical hydrodynamic model* to calculate the Marangoni force. At the beginning of the interfacial flow, the Marangoni force acts like a "hammer" and modifies the shape of the drop. This force also generates other various factors, like the surface dilution, the tip-stretching, and the capillary forces, that might appear in the drop dynamics, depending on the working conditions. The results of our theoretical hydrodynamic model are in a substantial agreement with the observed experimental data.

Under given conditions, tangential forces may exert in the interface of the two liquids, together with the normal pressure. If the surface tension, σ, of the liquid interface changes from point to point, a tangential force, $\vec{p}_t$, will be exerted in addition to the pressure normal to the surface and its magnitude is determined by the surface tension gradient, which per unit area is [7-12] (Eq. 1):

$$\vec{p}_t = grad\ \sigma \qquad (1)$$

The plus sign preceding the gradient indicates that this force tends to move the surface of the liquid in a direction from lower to higher surface tension (Figure 1). Surface active compounds, present in even small quantities, have an important role in determining the hydrodynamic behavior of the two-phase system. Those cases of liquid motion, in which surface tension plays an important role, belong to the interfacial hydrodynamics.

There are many examples where the presence of a surfactant has an important role. Probably, the best known is the effect of a surfactant on a liquid (L') free drop, immersed in an immiscible bulk liquid (L), initially at rest. The force, $\vec{F}$, acting on

the unit volume of the drop (density ρ') immersed in a bulk liquid (density ρ), is cancelled (Eq. 2):

$$\vec{F} = (\rho - \rho')\ \vec{g} = 0 \qquad (2)$$

either when the densities of the two liquids are equal (ρ' = ρ) or in the absence of gravity = 0 (zero gravity). Such a drop is called "free" and is motionless.
Free drops undergo complicated motion when a surface tension gradient is applied on the drop surface. Translational and rotational motion, oscillations, surface waves and deformations have been experimentally evidenced. To explain the free drop dynamics, we have developed some experiments and theoretical models [1–7]. We have shown that the *surface Marangoni flow* causes the motion of the neighboring liquids by viscous traction, which generates the force of hydrodynamic pressure, named *Marangoni force*.

The purpose of this work is to show, experimentally and theoretically, that this Marangoni force is correlated with the surface coverage degree, namely with the extent to which the drop surface is covered by the surfactant. Our calculations have shown that this force acts like a hammer and like an engine. So, we divided this force in:

- "hammer" force, responsible with the deformation and break-up of the drop, oscillations and surface waves, and
- "lifting" (propulsive) force, responsible with the translational motion of the drop.

Definitely, these results cannot be attribute to a single mechanism, in our case a mechanical one, but we might consider also other mechanisms, namely, the surface dilution and tip-stretching of the surface tension, as well as capillary forces. However, in our opinion, the real flow at the drop interface and consequently, the Marangoni force is the principal mechanism.

2. Experimental model

The investigation of the ***free drop dynamics*** is of a present interest, due to its appearance both in the industrial and biological processes, as well as in the space science and technology of liquids.

We shall consider a viscous (L') liquid drop (with density ρ') immersed in an unbounded immiscible (L) liquid (of density ρ) at a constant temperature (T); in our experiments with a volume between 0.4 cm^3 and 7 cm^3, noted L' of density ρ', immersed in an immiscible bulk liquid L of density ρ. The densities of the two bulk liquids (inside and outside the drop) are equal (ρ = ρ') and initially the drop is motionless. Such a drop is also called free drop. Further, we assume that both liquids

(L and L') are incompressible and Newtonians. The drop has a viscosity μ' and the surrounding bulk fluid a viscosity μ, which are, in general, different. The surface between the two bulk fluids is characterized by an interfacial tension noted σ_0.

Then, a small quantity of a surfactant (e.g., a droplet of 10^{-3}-10^{-2} cm^3, which is very small compared with the volume of the initial drop) is introduced on a well-chosen point (called also injection point) at the drop surface. Surfactants, also known as tensides, are wetting agents that lower surface tension of a liquid.

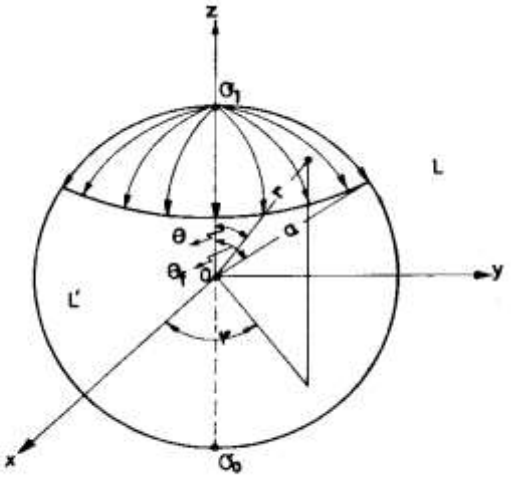

Fig. 2. The spreading and adsorption of a surfactant on the free drop surface; the system of spherical coordinates (r, θ, φ); the drop radius is noted *a*; the θ_f angle characterizes the position of the surfactant front. For symbols see the text.

The surfactant, because of its molecular structure, is spread and simultaneously adsorbed at the liquid-liquid interface and it is continuously swept along the meridians of the drop by the convective transport (see, Figure 2). In the injection point the interfacial tension is instantaneously lowered to σ_1 ($\sigma_1 < \sigma_0$) value. We mention that local changes in temperature [6-10] or the presence of surface chemical reactions might produce a similar effect.

Since the interfacial tension is a function of the surfactant concentration, a gradient of interfacial tension is established over the surface of the drop [3]. Consequently, the Marangoni spreading of the surfactant takes place from low surface tension to high surface tension (Figure 1). As a result of the Marangoni surface flow, which causes the motion of the neighboring liquids by viscous traction, the Marangoni force of hydrodynamic pressure will appear acting on the drop surface. Due to the drop symmetry, the Marangoni force has the application point in the injection point with surfactant at the drop surface.

This Marangoni force will determine all kinds of drop movements, especially deformations, rotations and oscillations of the whole drop, as well as surface waves and drop translational motions depending on the experimental working conditions. The symmetry of the problem suggests a system of spherical coordinates (r, θ, φ) with the origin placed in the drop center and with the Oz axis passing through the sphere in the point of the minimum interfacial tension, i. e., the injection point of the surfactant.

We underline that the surfactant injection point at the drop surface may be taken anywhere, the drop being initially at rest. In the following theoretical model, we shall take it like it is shown in Figure 2.

3. Variation of the Surface Tension

The variation of the interfacial tension over the drop surface must be defined before we can proceed with the analysis of the model. Generally, the interfacial tension, σ, is assumed to be distributed [9] within the surfactant invaded region, ($0 \le \theta \le \theta_f$), by

$$\sigma(\theta) = \sigma_m - a_1 \cos\theta$$

where σ_m and a_1 are constants.

For the variation of the interfacial tension with θ, we have proposed for the constant values:

$$\sigma_m = \frac{\sigma_0 - \sigma_1}{1 - \cos\theta_f} + \sigma_1 \quad \text{and} \quad a_1 = \frac{\sigma_0 - \sigma_1}{1 - \cos\theta_f}.$$

Thus, the above equation becomes:

$$\sigma(\theta) = \frac{\sigma_0 - \sigma_1}{1 - \cos\theta_f}(1 - \cos\theta) + \sigma_1 \qquad (1)$$

where $\sigma_0 = \sigma(\theta_f)$ and $\sigma_1 = \sigma(0)$.

The surfactant front position, in this radial flow, is noted by the angle θ_f, and the interfacial tension, σ, is considered a unique function of the angle θ. Within the surfactant invaded region, ($0 \le \theta \le \theta_f$), for the variation of the interfacial tension with θ, we take the equation (1).

Equation (1) presents the advantage that it contains the angle θ_f and permits the calculation of σ for different drop coverage with surfactant. For the situation when the surface of the entire drop is covered with surfactant, $\theta_f = \pi$, Eq. (1) is similar to that one proposed by other authors [10]. This confirms that Eq. (1) proposed by us in its general form is correct. Further, by derivation of Eq. (1), the interfacial tension gradient, $d\sigma/ d(\theta)$, in the invaded drop region, Figure 2, with surfactant is obtained:

$$\frac{d\sigma}{d\theta} = \frac{\sigma_0 - \sigma_1}{1 - \cos\theta_f} \sin\theta, \tag{2}$$

where, the interfacial tension σ_0 is constant in any point of the uncovered drop surface, while the interfacial tension difference $\Pi = \sigma_0 - \sigma_1$ arises only in the invaded region with surfactant. Therefore, it is clear that only σ_1 and σ_0, *i.e.,* the minimum and the maximum values of the interfacial tension, can be experimentally measured.

4. Theoretical Model

4.1. Theoretical framework for surface-driven fluid motion in sessile drops

The ***theoretical model*** reported here considers that the drop is initially at rest and the real surface flow – Marangoni flow – arises on the drop surface, with a distinct front, which advances continuously; without a surfactant transfer inside or outside the drop. The drop surface is considered a two-dimensional, incompressible Newtonian fluid. The Reynolds number of the inside and outside flow is less than unity. The equations governing the flow inside and outside the drop are the continuity and Navier-Stokes equations [11-13]. The continuity equations for a Newtonian incompressible fluid, for the outside and inside flow are as given by Eqs. (3, 4):

$$\nabla \cdot \vec{v} = 0, \tag{3}$$

$$\nabla \cdot \vec{v}' = 0, \tag{4}$$

where $\vec{v}$ is the velocity of the bulk liquid L and $\vec{v}$ ' represents the velocity of the liquid L' within the drop.

The Navier-Stokes equations for a steady flow are as follows (Eqs. 5, 6):

$$(\vec{v} \cdot \nabla)\, \vec{v} = -\frac{1}{\rho} \text{grad}\, p + \nu \Delta \vec{v}, \tag{5}$$

$$(\vec{v}' \cdot \nabla)\, \vec{v}' = -\frac{1}{\rho} \text{grad } p' + \nu' \Delta \vec{v}', \qquad (6)$$

where *p* and *p'* are the pressures outside and inside of the drop; $\nu = \frac{\mu}{\rho}$ and $\nu' = \frac{\mu'}{\rho}$ are the kinematic viscosities of continuous liquid and drop liquid, respectively.

All these parameters are considered constants. We propose here to give some account on the equations governing the fluid motion in a surface, considered as a two-dimensional, incompressible Newtonian fluid, having surface density, Γ, surface dilatational κ viscosity and surface shear ε viscosity. Even that we consider the interface like a bi-dimensional geometrical surface, it has a finite thickness about 5 x10^{-10} cm.

The flow in a surface is not just a flow in a two-dimensional space whose governing equations will be immediate analogs of the three-dimensional ones. In contrast with the three-dimensional space, this surface is a two-dimensional space that moves within a three-dimensional space surrounding it. In our case, the interface is the region of contact of two liquids, i.e. drop liquid and bulk liquid. This is a new feature which oblige us to take account on the dynamical connection between the surface and its surroundings, namely on the traction exerted by the outer $\vec{T}$ and inner $\vec{T}'$ liquid upon the drop interface.

The equation of the interfacial flow [14-17] is (Eq. 7):

$$\Gamma\left(\vec{w} \cdot \nabla_S\right)\vec{w} = \vec{F} + \nabla_S \sigma + \left(\kappa + \varepsilon\right)\nabla_S\left(\nabla_S \cdot \vec{w}\right), \qquad (7)$$

where $\vec{w} = \vec{v}_S$ is the interface velocity, $\vec{F} = \Gamma \vec{g} + \vec{T} - \vec{T}'$ is the external force acting on the drop surface, and ∇_S is the surface gradient operator. Because the surface density [16] is very small ($\Gamma \approx 10^{-7}$g cm^{-2}) the inertial term can be neglected against the remainder terms. It is significant to underline that equation (7) can be used in two ways: as the equation which describes the surface flow or as a dynamical boundary condition.

In order to find the distributions of the velocities $\vec{v}$ and $\vec{v}'$ and of the pressures p and p', the system of equations (3)-(7) must be solved taking into account some appropriate boundary conditions [11- 13].

Thus, the velocities of the inner and outer liquid of the drop must satisfy the following kinematical conditions:

- the outer velocity must be zero far from the drop surface,
  $\vec{v} = 0$ for $r \to \infty$;

- the normal component of the outer and the inner velocities must be zero on the surface of the drop

  $\vec{v}_n = \vec{v}_n' = 0$, at r = a;

- the tangential velocity components of the two liquids at the interface must be equals

  $\vec{v}_t = \vec{v}_t'$ at r = a;

- the velocity $\vec{v}'$ within the drop must remain finite at all points, particularly at the centre of the drop (r = 0, the origin of the coordinates).
- In addition to these kinematical conditions, a dynamical condition must be fulfilled at the interface and is given by Eq. (7). Eqs. (3–7) with these appropriate boundary conditions lead to the distribution of the velocity, $\vec{v}$, and of the pressures, p, outside of the drop. Similar expressions for the inner flow are obtained.

4.2. Marangoni flow

Since the ***Marangoni flow*** on the surface of the drop r = a is symmetrical with respect to the Oz axis, the velocities of the inner and outer liquid flows are not functions of the angle φ, they will have only normal (radial) and tangential components $v_r(r,\theta), v_r'(r,\theta), v_\theta(r,\theta), v_\theta'(r,\theta)$.

The continuity equation (3) for the outer flow in spherical coordinates is as given by Eq. (8).

$$\frac{\partial v_r}{\partial r} + \frac{1}{r}\frac{\partial v_\theta}{\partial \theta} + \frac{2v_r}{r} + \frac{v_\theta \operatorname{ctq}\theta}{r} = 0, \tag{8}$$

while for the Navier-Stokes equations (5) and (6), we have Eqs. (9, 10).

$$\frac{\partial p}{\partial r} = \mu\left(\frac{\partial^2 v_r}{\partial r^2} + \frac{1}{r^2}\frac{\partial^2 v_r}{\partial \theta^2} + \frac{2}{r}\frac{\partial v_r}{\partial r} + \frac{\operatorname{ctg}\theta}{r^2}\frac{\partial v_r}{\partial \theta} - \frac{2}{r^2}\frac{\partial v_\theta}{\partial \theta} - \frac{2v_r}{r^2} - \frac{2\operatorname{ctg}\theta}{r^2}v_\theta\right) \tag{9}$$

$$\frac{1}{r}\frac{\partial p}{\partial \theta} = \mu\left(\frac{\partial^2 v_\theta}{\partial r^2} + \frac{1}{r^2}\frac{\partial^2 v_\theta}{\partial \theta^2} + \frac{2}{r}\frac{\partial v_\theta}{\partial r} + \frac{\operatorname{ctg}\theta}{r^2}\frac{\partial v_\theta}{\partial \theta} + \frac{2}{r^2}\frac{\partial v_r}{\partial \theta} - \frac{v_\theta}{r^2 \sin^2\theta}\right) \tag{10}$$

It is to be noted that similar equations are obtained for the inner liquid motion. The velocities of the inner and outer flow satisfy the following boundary conditions (Eqs. 11-14).

$$v_r = v_\theta = 0 \quad \text{for} \quad r \to \infty, \tag{11}$$

$$v_r = v_r' = 0 \quad \text{at} \quad r = a, \tag{12}$$

$$v_\theta = v_\theta' \quad \text{at} \quad r = a \ , \tag{13}$$

$$v_r' \text{ and } v_\theta' \quad \text{finite at} \quad r = 0 \ . \tag{14}$$

In addition to these kinematic conditions, we also have, as we pointed before, a dynamic condition on the drop surface (r = a), obtained from the interface flow equation (7), which for small interfacial density Γ can be written in the following form [14,15] (Eq. 15):

$$\mu\left(\frac{1}{r}\frac{\partial v_r}{\partial\theta} + \frac{\partial v_\theta}{\partial r} - \frac{v_\theta}{r}\right)_{r=a} + \frac{1}{a}\frac{d\sigma}{d\theta} + (\kappa+\varepsilon)\left[\frac{1}{r}\frac{\partial}{\partial\theta}\left\{\frac{1}{r\sin\theta}\frac{\partial}{\partial\theta}(v_\theta\sin\theta)\right\}\right]_{r=a} \tag{15}$$

$$+\varepsilon\frac{2(v_\theta)_{r=a}}{a^2} = \mu'\left(\frac{1}{r}\frac{\partial v_r'}{\partial\theta} + \frac{\partial v_\theta'}{\partial r} - \frac{v_\theta'}{r}\right)_{r=a} .$$

4.3. Solution of the flow equations

The solution of the flow equations (8-10) with the boundary conditions (11-15) can be obtained if we note that the surface flow gives rise to a current fluid directed to the drop along the Oz axis. This current fluid arises as a consequence of the continual replacement, by a ventilation effect, of that liquid layer which it was displaced by the interfacial flow. The profile of the flow indicates that a solution of the flow equations should be sought [13] in the form:

$$\begin{aligned} v_r(r,\theta) &= f(r)\cos\theta, \\ v_\theta(r,\theta) &= g(r)\sin\theta, \\ p(r,\theta) &= \mu\, h(r)\cos\theta, \end{aligned}$$

for the outer liquid L, and similar Eqs. are obtained for the inner liquid L'.

After well-known manipulations, we obtain for f, g, and h, the following relations:

$$f(r) = \frac{b_1}{r^3} + \frac{b_2}{r} + b_3 + b_4 r^2,$$

$$g(r) = \frac{b_1}{2r^3} - \frac{b_2}{2r} - b_3 - 2b_4 r^2 ,$$

$$h(r) = \frac{b_2}{r} + 10 b_4 r,$$

with b_1, b_2, b_3 and b_4 as constants. Also, equations of identical form for f', g' and h' are obtained with constants b_1', b_2', b_3', b_4'.

The eight b unknown constants will be determined from the boundary conditions (11-15). From Eqs. (11) and (14), we have can find: $b_3 = b_4 = b_1' = b_2' = 0$. For the outer liquid motion, we obtain:

$$v_r(r,\theta) = \left(\frac{b_1}{r^3} + \frac{b_2}{r}\right)\cos\theta,$$

$$v_\theta(r,\theta) = \left(\frac{b_1}{2r^3} - \frac{b_2}{2r}\right)\sin\theta,$$

$$p(r,\theta) = \mu\frac{b_2}{r^2}\cos\theta,$$

and for the velocity and pressure distribution within the drop

$$v_r'(r,\theta) = (b_3' r^2 + b_4')\cos\theta,$$

$$v_\theta'(r,\theta) = -(2b_3' r^2 + b_4')\sin\theta,$$

$$p'(r,\theta) = 10\mu' b_3' r\cos\theta.$$

From Eqs. (12) and (13) we have:

$$b_2 = -\frac{b_1}{a^2},\quad b_3' = -\frac{b_1}{a^5},\quad b_4' = \frac{b_1}{a^3}.$$

Then, from equation (15), where for $\frac{d\sigma}{d\theta}$ we have used equation (2), the dependence of the constant b_1 as a function of the interfacial tension gradient $\Pi = \sigma_0 - \sigma_1$ is obtained:

$$b_1 = \frac{(\sigma_0 - \sigma_1)a^3}{3(\mu + \mu' + 2\kappa/3a)(1 - \cos\theta_f)}.$$

Thus, Eqs. (8-10) with the appropriate boundary conditions (11-15) lead to the distribution of the velocities $\vec{v}, \vec{v}'$ and of the pressures p, p' outside and inside the drop (Eqs. 16-18):

$$v_r(r,\theta) = \frac{(\sigma_0 - \sigma_1)a^3}{3(\mu + \mu' + 2\kappa/3a)(1-\cos\theta_f)}\left(\frac{1}{r^3} - \frac{1}{a^2 r}\right)\cos\theta, \quad (16)$$

$$v_\theta(r,\theta) = \frac{(\sigma_0 - \sigma_1)a^3}{3(\mu + \mu' + 2\kappa/3a)(1-\cos\theta_f)}\left(\frac{1}{2r^3} + \frac{1}{2a^2 r}\right)\sin\theta, \quad (17)$$

$$p(r,\theta) = -\frac{\mu(\sigma_0 - \sigma_1)a}{3r^2(\mu + \mu' + 2\kappa/3a)(1-\cos\theta_f)}\cos\theta, \quad (18)$$

for the outer flow, and equations (19-21) for the inner flow.

$$v_r'(r,\theta) = \frac{\sigma_0 - \sigma_1}{3(\mu + \mu' + 2\kappa/3a)(1-\cos\theta_f)}\left(1 - \frac{r^2}{a^2}\right)\cos\theta \quad (19)$$

$$v_\theta'(r,\theta) = -\frac{\sigma_0 - \sigma_1}{3(\mu + \mu' + 2\kappa/3a)(1-\cos\theta_f)}\left(1 - \frac{2r^2}{a^2}\right)\sin\theta \quad (20)$$

$$p'(r,\theta) = -\frac{10\,\mu'(\sigma_0 - \sigma_1)r}{3\,a^2(\mu + \mu' + 2\kappa/3a)(1-\cos\theta_f)}\cos\theta \quad (21)$$

4.4. Marangoni force, $F_M(\theta_f)$, exerted on the free drop

4.4.1. Calculation and Angular Dependence of the Marangoni Force on the Drop Interface

Further, we describe the ***Marangoni force F_M exerted*** on the free drop due to *Marangoni flow*. If we analyze the model of the *Marangoni interfacial flow*, we find that as the flow occurs with the driving by viscosity, of the outer liquid L, the forces of hydrodynamic pressure will act on the drop L'. The resultant of the forces exerted by the outer fluid on the drop, F_M, due to the symmetry of the Marangoni flow, is oriented along the Oz axis. This force, acting on the drop, can be calculated from the general expression of the force given in [11] (Eq. 22):

$$F_M = \iint_S (p_{rr}\cos\theta - p_{r\theta}\sin\theta)\, ds \quad (22)$$

where S is the surface covered with surfactant, and p_{rr} and $p_{r\theta}$ are the normal and tangential components [11-13], respectively, of the viscous stress tensor given by Equations (23, 24):

$$p_{rr}(r,\theta) = -p + 2\mu \frac{\partial v_r}{\partial r}, \tag{23}$$

$$p_{r\theta}(r,\theta) = \mu\left(\frac{1}{r}\frac{\partial v_r}{\partial \theta} + \frac{\partial v_\theta}{\partial r} - \frac{v_\theta}{r}\right). \tag{24}$$

The surface element, ds, in spherical coordinates on the drop (r = a) is:

$$ds = 2\pi a^2 \sin\theta \, d\theta,$$

and, the force acting on the drop, F_M, given by Eq. (22), can then be rewritten as given by Eq. (25):

$$F_M(\theta_f) = 2\pi a^2 \int_0^{\theta_f} (p_{rr}\cos\theta - p_{r\theta}\sin\theta)\sin\theta \, d\theta \, . \tag{25}$$

Using Eqs. (16-18), one obtains for the normal (Eq. (23) and tangential (Eq. (24) components of the stress tensor, at the drop surface (r = a), the following expressions [9, 17] (26, 27):

$$(p_{rr})_{r=a} = -\frac{\mu(\sigma_0 - \sigma_1)}{a\left(\mu + \mu' + 2\kappa/3a\right)(1-\cos\theta_f)}\cos\theta, \tag{26}$$

$$(p_{r\theta})_{r=a} = -\frac{\mu(\sigma_0 - \sigma_1)}{a\left(\mu + \mu' + 2\kappa/3a\right)(1-\cos\theta_f)}\sin\theta \, . \tag{27}$$

Introducing the viscosities ratio, $\lambda = \mu'/\mu$, the interfacial tension difference, $\Pi = \sigma_0 - \sigma_1$, and because $2\kappa/3a \approx 0$ as shown previously [5, 18-25], after the integration of Eq. (25), by using Eqs. (26) and (27), the force acting on the drop surface, $F_M(\theta_f)$, is given by the following expression (eq. 28):

$$F_M(\theta_f) = C\,(1 - 2\cos\theta_f - 2\cos^2\theta_f), \tag{28}$$

where C is given as A/3, where A is specified as $A = \frac{2\pi a \Pi}{1+\lambda}$.

Thus, Eq. (28) represents the Marangoni force acting on the drop surface along the Oz axis. It can be seen that this force depends on the θ_f angle, namely, on the extent

to which the drop surface is covered by the surfactant, as a function of the radial interfacial tension difference (Π), the ratio of the bulk viscosities (λ), as well as of the radius (a) of the drop.

4.4.2. Hammer Effect: Marangoni hammer force and Marangoni lifting force

For further discussions, it is useful to introduce a new function in Eq. (28), namely $f(\theta_f) = F_M(\theta_f)/C = F_m(\theta_f)$, given by:

$$f(\theta_f) = 1 - 2\cos\theta_f - 2\cos^2\theta_f \qquad (29)$$

which is plotted in Figure 3.

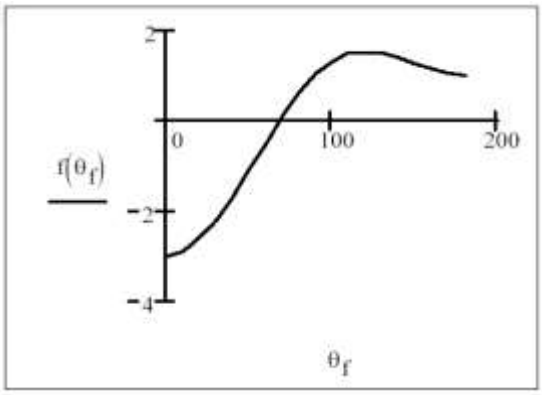

Fig. 3. The graphic of the $f(\theta_f)$ as a function of θ_f angle (^{0});
$f(\theta_f) = F_m(\theta_f) = F_M(\theta_f)/C$.

The value of θ_f, for which the force $F_M(\theta_f)$ cancels, $F_M(\theta_f) = 0$, is $\theta_0 \approx 68.53^0$. The value of θ_0 does not depend on the physical, chemical and geometric properties of the drop. Also, we see that for $\theta_f \in [0, \theta_0)$, the force is negative $F_M(\theta_f) < 0$, and for $\theta_f \in (\theta_0, 180^0]$ the force is positive, $F_M(\theta_f) > 0$, having the greatest value for $\theta_m = 120^0$.

From Eq. (28) it is found that for a coverage degree $\theta_f < \theta_0$ of the drop, with surfactant, as a result of the appearance of a radial interfacial tension gradient Π, the pressure force $F_M(\theta_f)$ exerted by the external liquid upon the drop is oriented toward the negative direction of the Oz axis (Figure 3). This is similar with the application of a "hammer" knock on the drop in the injecting point of the surfactant.

For a coverage degree θ_f greater than θ_0, but less than 180^0, the force $F_M(\theta_f)$ is oriented towards the positive direction of the Oz axis. The propulsive (lifting) force, $F_M(\theta_f) > 0$, responsible for the upward movement of the drop, appears only when the coverage of the drop with surfactant is greater than θ_0.

Therefore, the effect of coverage by the surfactant on the drop surface can be decomposed in two parts, the "hammer" effect for the coverage $0 \leq \theta_f < \theta_0$ and the "propulsive" effect for the coverage $\theta_0 < \theta_f \leq 180^0$ as shown in Figure 4a and Figure 4b, respectively.

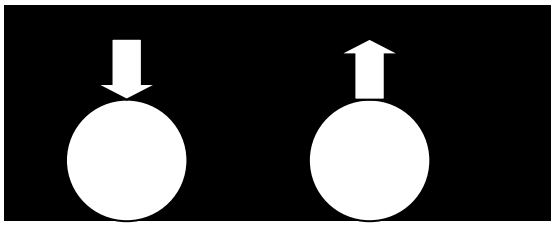

(a) (b)

Fig. 4. The Marangoni force, FM, acting on the free drop. a) Marangoni hammer force; b) Marangoni lifting force.

Furthermore, the normal force acting on the interface will tend to deform the drop from a spherical shape [17, 25-29]. So, the principal mechanical factor which can modify the shape of the drop, namely deformations and break-ups of a drop, is the normal component of the Marangoni force (Figure 3).

To understand better the role of this force, on the deformations of the drop, it will be useful to calculate the normal F_n component of the resultant force F_M.

4.4.3. $F_M(\theta_f)$ force and its maximum

The normal component F_n of the force F_M is given by:

$$F_n(\theta_f) = C\,(-1 - \cos\theta_f - \cos^2\theta_f). \qquad (30)$$

It can be understood that this force F_n depends on the θ_f angle, namely on the extent to which the drop surface is covered by the surfactant, the interfacial tension difference, Π, and the ratio of the bulk viscosities, λ. The normal component of Marangoni force (in short, the normal force) is negative and consequently acts in the opposite direction of the normal at the drop surface (Figure 2 and Figure 4a) for any degree of coverage with surfactant.

Also, it can be observed from Eq. (30) that this component is at its minimum for $\theta_f = 0$ (i.e. at the point of the surfactant injection) and increases rapidly but it never reaches positive values for any value of θ_f.

The maximum magnitude of the normal force is for $\theta_f = 0$ and is given by:

$$F_n(0) = - [A = \frac{2\pi a \Pi}{1+\lambda}] \qquad (31)$$

Further, it is to be noted that $F_n(0) = F_M(0)$ (in absolute value). The normal force acts like a hammer (hammer effect, Figure 4a), deforming or even breaking up the drop, for any value of θ_f between 0 and π.

As shown by Eq. (31), the hammer effect appears directly proportional with the surface tension effects, Π, and with the radius (a) of the drop and inversely proportional to λ.

The tangential component, F_t, of the Marangoni force, or tangential force, is responsible for translational motion of the drop and it is given by the following expression:

$$F_t(\theta_f) = C (2 - \cos\theta_f - \cos^2\theta_f) \qquad (32)$$

where C is given as A/3.

The tangential force F_t is positive for any value of θ_f between 0 and π, namely for any extent of coverage with surfactant on the drop surface. It is found, from Eq. (32), that the tangential force F_t is practically zero for small value of θ_f, having a maximum value at $\theta_f = 2\pi/3$. The resultant force, noted $f(\theta_f) = F_M(\theta_f)/C$, is given as a function of θ_f angle in Figure 3, and it has two components, normal force, $F_n(\theta_f)/C$, and tangent, $F_t(\theta_f)/C$, force. The resultant force, $f(\theta_f)$ can be noted also as F_m, which is F_M/C, and it vanishes for $\theta_0 \approx 7\pi/18$ ($\approx 68.53°$).

It is to be noted that, for any degree of coverage, $\theta_f < \theta_0$, with surfactant, the resultant F_m force exerted by the external liquid upon the drop is oriented towards the negative direction of the Oz axis.

At greater surfactant coverage degree of the drop surface, at $\theta_f > \theta_0$, although F_n is not zero, the tangent force F_t is much larger than the absolute value of the normal force, so the resultant force F_M is positive. In other words, the normal force and the tangent force do not cancel out for any value of θ_f and consequently the resultant force F_M changes its sign, as shown in Figure 3. Evidently, the $F_M(\theta_f)$ force reaches its maximum value at the spreading moment of the surfactant (t=0) for which $\theta_f \approx 0$ and is given by (Eq. 33):

$$F_M(0) = A \text{ (where } A=\frac{2\pi a \Pi}{1+\lambda} \text{)} \quad (33)$$

where $F_M(0)$ represents *the resultant force acting on the drop surface* in the injecting point.

For physical meanings, we can take the absolute value of this Marangoni hammer force.

4.5. Drop deformation

In our opinion, the Marangoni hammer force is the principal factor which can modify the shape of the drop, namely through deformations and breakups of a drop. It is valued to point out the importance of *Marangoni hammer force* and *Marangoni surface flow*, which are at the origin of other interfacial processes [18-40]. Indeed, the modification of the surface area of a drop, when the drop is deformed to a non-spherical shape, dilutes the surfactant surface concentration and the deformation of the drop is different from that expected one for the equilibrium σ_0 case. This is called the ***surface dilution effect.***

Also, especially at the break-up process of the drop, surfactant molecules may accumulate at the tip of the drop due to the convection phenomenon. This phenomenon decreases the local interfacial tension and causes the tip to be overstretched. This process is called the ***tip-stretched effect.*** During deformations, when a drop gets a concave surface, capillary forces appear, which tend to bring the drop in the initial spherical shape. All these effects can appear, as a consequence of the Marangoni hammer force and due to the real flow of surfactant molecules on the drop surface.

Therefore, we suggest that the primary effect, due to a reduction of the equilibrium interfacial tension (σ_0) in the injection point of a free drop surface with a surfactant, at $t=0$, is the appearance of a Marangoni surface flow of the surfactant on the drop surface. This Marangoni flow of the surfactant modifies the equilibrium surface tension, σ_0, and a Marangoni force $F_M(\theta_f)$ will act on the drop. At the beginning, it acts like a hammer which changes the shape of the drop, and consequently, several factors might appear, namely, the surface dilution and tip-stretching, as well as capillary forces.

4.6. Internal wave trains

Further, we suggest that it is a direct connection between Marangoni force and the deformation of the drop, via the *surface waves* produced by the *hammer effect*. Furthermore, we have considered that the surface waves, generated by the hammer effect, produce traveling periodic internal wave trains [28-32]. If these internal waves are absorbed by drop, the shape of the drop is not deformed. If these internal

waves are not absorbed, the overlapping of the direct and reflected internal waves modifies the shape of the drop and causes deformations or even the break-up of the drop. For small surface tension gradients, even in the case of the drop not deformable, there are different movements, first of all, the surface waves.

We suggest that these surface waves are produced by the hammer effect described above. The surface waves generate a surface Marangoni instability of the drop. This instability was observed previously [23] but its cause was not discovered.

Our theoretical model can describe the surface instability due to the hammer effect. Further on, these *surface waves* will produce *the internal waves* which are generated by the surface tension gradients through hammer impact. As a consequence, traveling periodic internal wave trains are generated in the liquid drop after the adsorption and spreading of the surface-active compound on the surface of the drop, as illustrated latter on in the experimental work [25-32].

Further, two possibilities can occur for the hammer effect for $\theta_f \leq \theta_0$:

1. If the drop viscosity μ' is big, then, the energy of the traveling periodic *internal trains of waves* are absorbed by the drop liquid and the drop is not deformable. Nevertheless, other movements might appear, like oscillations of the whole drop and rotations.
2. When the drop viscosity μ' is small and the energy of the internal waves is not absorbed, the waves are reflected by the internal drop surface. The superimposing of the direct internal waves with the reflected ones gives a rise to a "resonant" effect, which generates the deformation and even break-up of the drop.

5. Experimental Section

The experimental work on drop dynamics and Marangoni instability was performed in liquid-liquid systems of equal densities presented in Tables 1 and 2. The densities of the liquids were determined picnometrically and the bulk viscosities by using an Ubbelohde viscometer. The surface dilatation viscosity at the liquid/liquid interface was not directly measured and only a few indications concerning this magnitude for the liquid/gas interface have been found [3, 4, 6, 17, 25, 26].

The mixtures, making up the continuous L phase, were placed in a thermostated parallelepiped vessel of 1 dm^3, made of transparent glass. The drop (L') was made of various radii between 0.46 and 1.19 cm, by using the mixtures described in Table 1. The L' liquid was carefully submerged by using a pipette into the continuous L aqueous phase and the density of the latter was then adjusted by adding small quantities of water or alcohol until the buoyancy of the drop practically disappeared. After the system was stabilized, a small quantity (10^{-3}-10^{-2} cm^3) of the surfactant

solution (Ss) was injected with a micrometric syringe, in a point on the drop surface (injection point in Figure 2).

The injection was done either in a vertical direction (as in Figure 5) or in different directions (Figures 6 and 7) and no influence of the mode of injection on the Marangoni flow or on the drop movements and deformations were observed.

The interfacial tension of the liquid/liquid systems, e.g., L/L', was determined by a method based on capillarity [3] and its value is given in Table 2. The measurement of the above parameters as well as the drop dynamics and surface flow experiments have been performed at constant temperature (20 ± 0.1^{o} C). All chemicals were of analytical purity and used without further purification. In order to make visible the surface flow, the surfactant solution was intensely colored with methylene blue (0.28 g/100 cm^3). Surfactants were soluble in the continuous phase L for system 1. For the 2 and 3 systems, the surfactant was insoluble both in the L and L' liquid phases.

The movement of the surfactant front was followed by filming with a high-speed camera (500 images/sec). A number of sequences, showing the surfactant front position at various moments, t, of the process, is presented in Figure 5. It can be seen that the front position is easily distinguishable from the uncovered drop surface.

The positioning of the L' liquid drop in the continuous L liquid for a sufficiently long time, as to perform the flow measurements, raises difficulties. Although some authors pointed out that two drops never behave in the same manner under the action of interfacial tension differences, we have succeeded in measuring the reproducible surface flow velocities as well as in evidencing the influence of several factors, like interfacial tension gradients and viscosities, on the drop deformations and drop movements.

6. Results and Discussion

The composition and physical characteristics of the liquid/liquid (L/L') systems, of equal densities, are given in Table 1. Bulk viscosities μ and μ', and interfacial tensions σ_0 and σ_1, are also presented in Table 1.

The values of the surface tension gradient, Π, the ratio of the viscosities, $\lambda = \mu'/\mu$, and the Marangoni hammer $F_M(0)$ force (see, equation 33) are given in Table 2.

The experimental parameters are presented for three different cases of drop dynamics, under various surface tension gradients Π. The first case (system 1) corresponds to the nondeformable drop (Figure 5). The second case (system 2) represents the situation of the deformable drops (Figure 6) and the third one (system 3) describes the breakup of a free drop (Figure 7).

For system 1, the drop radius is a = 1.19 cm and for systems 2 and 3, the drop radius is a = 0.46 cm (Table 1).

Table 1. The composition and physical characteristics of the liquid/liquid (L/L') systems of equal densities and for surfactant solution (Ss).

System No.	*Continuous Phase (**L**)*			*Drop Phase (**L'**)*		*Surfactant Solution (**Ss**)*	
	Composition (% volume)	μ (cP)	σ_0 L / L' dyn/cm	Composition (% vol)	μ' (cP)	Composition (% volume)	σ_1 L' / S dyn/cm
1	Methanol 78 Water 22	1.33	10.2	Paraffin oil	80	Propanol 77.3 Water 22.7	3.5
2	$NaNO_3$ 15.1 Water 84.9	1.10	28.2	Chlorobenzene 50 Silicon oil 50	5.46	Benzyl alcohol 89 CCl_4 11	3.6
3	$NaNO_3$ 14.9 Water 85.1	1.10	22.8	Chlorobenzene 92 Silicon oil 8	1.03	Benzyl alcohol 89 CCl_4 11	3.6

Table 2. Surface tension gradients, $\Pi = \sigma_0 - \sigma_1$, the ratio of the viscosities, λ, and the calculated values of Marangoni hammer force $F_M(0)$, for the three systems.

System No.	*Π (dyn/cm)*	*λ*	*$F_M(0)$, (dyn)*	*Remarks*
1	6.7± 0.3	60.15	0.82	The free drop remains practical nondeformable and the translational motion is insignificant (Fig. 5).
2	24.6± 0.3	4.96	11.92	The free drop might have slight or big deformations (Fig. 6), but after 0.8 s, it returns (Fig. 6e) to its initial shape (Fig. 6a). The translational motion (Fig. 6e) is evident from the initial position (Fig. 6a); drop deformation (Fig. 6b); drop rotation is observed in Fig. 6c and Fig. 6d against Fig. 6a.
3	19.2± 0.3	0.94	28.57	The free drop, Fig. 7, drop deformation, Fig. 7b, c, d, after 0.3-0.4 s, drop breaks up into two droplets Fig. 7e, f, which are also moving, as evidenced in Fig. 7d against initial Fig. 7a.

Then, we compare the calculated values, obtained with our *hydrodynamic theoretical model*, with some experimental observations on the deformations and the break-ups of the drops under the *surface tension gradient.*

The drops were visualized by filming with a high-speed camera (500 images/sec). A number of image sequences illustrating the deformations of the drop at various moments (at different times, t) are presented in Figure 6 and of the break-up in Figure 7. In Figure 5, the filmed drop images, at different moments of time (t), are shown for the case of a nondeformable free drop. In these images is possible to observe the motion of the surfactant front on the drop surface, easily distinguishable, by the contrast with the uncovered drop surface. Also, in Figure 5, we can observe that the horizontal line, corresponding for the initial position of the free drop, is only slightly modified in time and the drop is not deformed or moved.

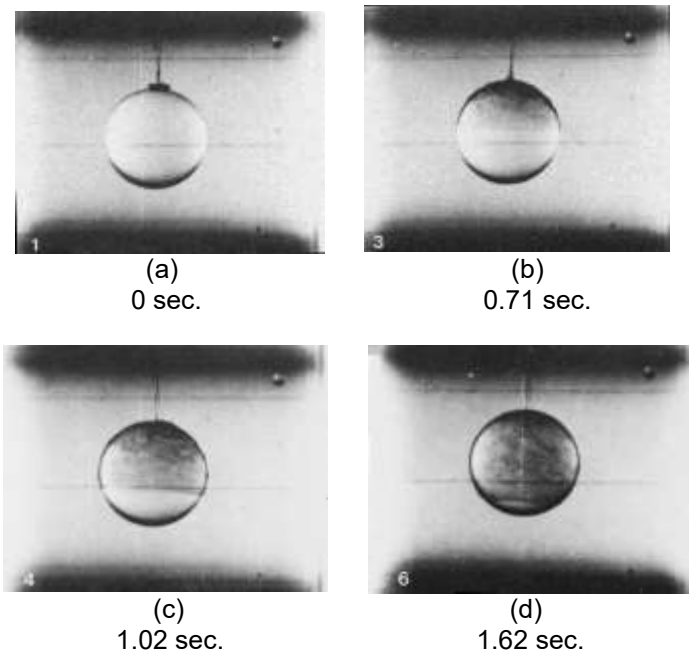

Fig. 5. Filmed pictures of a nondeformable drop characterized by the system 1, given in Tables 1 and 2; the interfacial tension difference, $\Pi = \sigma_0 - \sigma_1 = 6.7$ dyn/cm, the viscosities ratio $\lambda = 60.15$, a = 1.19 cm, and the calculated Marangoni force, $F_M(0) = 0.82$dyn.

These findings are in substantial agreement with the data earlier published [3], for nondeformable free drops. For comparison, we have chosen similar experimental conditions given in Table 1, for system 1 and therefore, we clearly demonstrated the reproducibility of these experiments. In plus, here, we calculated the Marangoni force $F_M(0)$, which is given in Table 2.

The normal force acts like a hammer (hammer effect), deforming and even breaking up the drop. As shown by Eq. (33), the hammer effect appears directly proportional with Π and with the radius (a) of the drop and inversely proportional to λ. Therefore, at big values of λ ratio (Figure 5, Table 2), the Marangoni force is small and a significant deformation and the displacement of the drop, after the surfactant injection, are not observed. However, the normal force may produce some gentle surface waves, but these waves were not detectable in these experimental conditions.

Then, we compare the calculated values, obtained with our *hydrodynamic theoretical model*, with some experimental observations on the deformations and the break-ups of the drops under the *surface tension gradient.* The drops were visualized by filming with a high-speed camera (500 images/sec). A number of image sequences illustrating the deformations of the drop at various moments (at different times, t) are presented in Figure 6 and of the break-up in Figure 7.

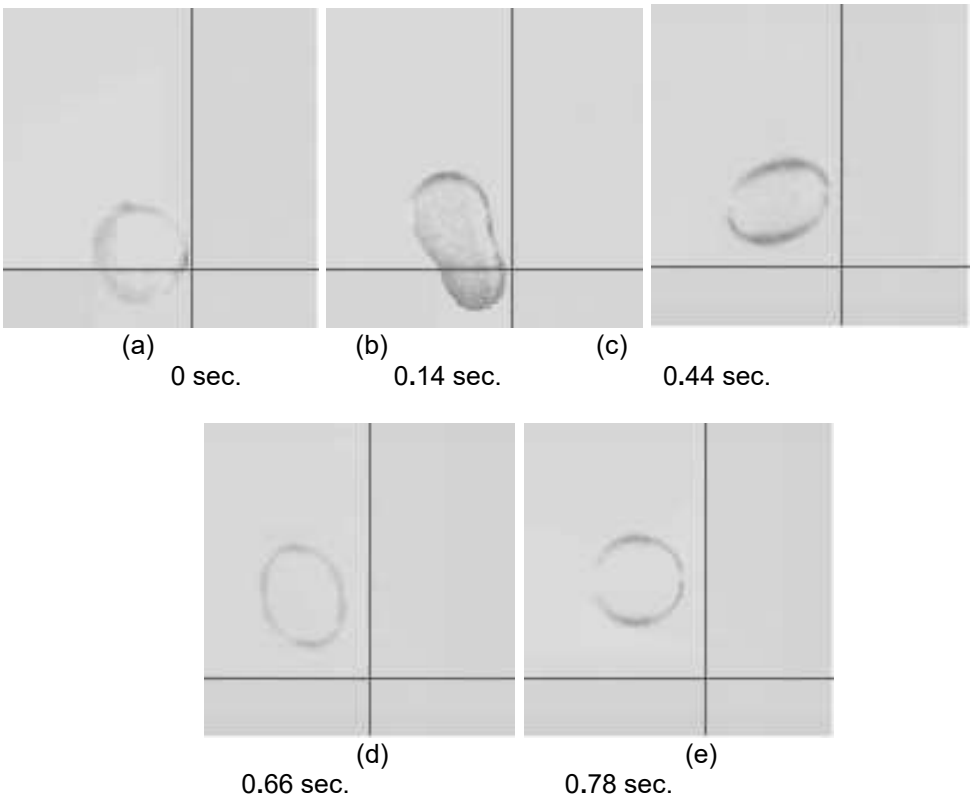

Fig. 6. Filmed pictures of drop deformations. The liquid-liquid (L/L') system is characterized by the system 2 in Tables 1 and 2; Π =24.6 dyn/cm; λ = 4.96; a = 0.46 cm; $F_M(0)$ = 11.92 dyn.

Figure 6 shows different shapes of a deformable free drop, Figure 6a-d, and its movement from the initial position (i.e., from the shown reference horizontal line). In this case, for the system 2, given in Tables 1 and 2, due to the variation of the drop shape, besides the Marangoni force, the surface dilution and capillary forces will appear in the description of drop deformations.

At the surfactant injection moment, the resultant Marangoni force F_m is negative (Figure 3), acting on the opposite direction of the normal to the drop surface and having its effect as the changing of the drop shape, e.g., Figure 6b compared to Figure 6a. For $\theta_f > \theta_0$ the resultant F_m force becomes positive and its effect is the propulsion of the drop or the translational movement of the drop along the Oz axis (Figures 6c, 6d); after 0.78 s, the free drop has its initial shape in Figure 6e, with its displacement on Oz axis.

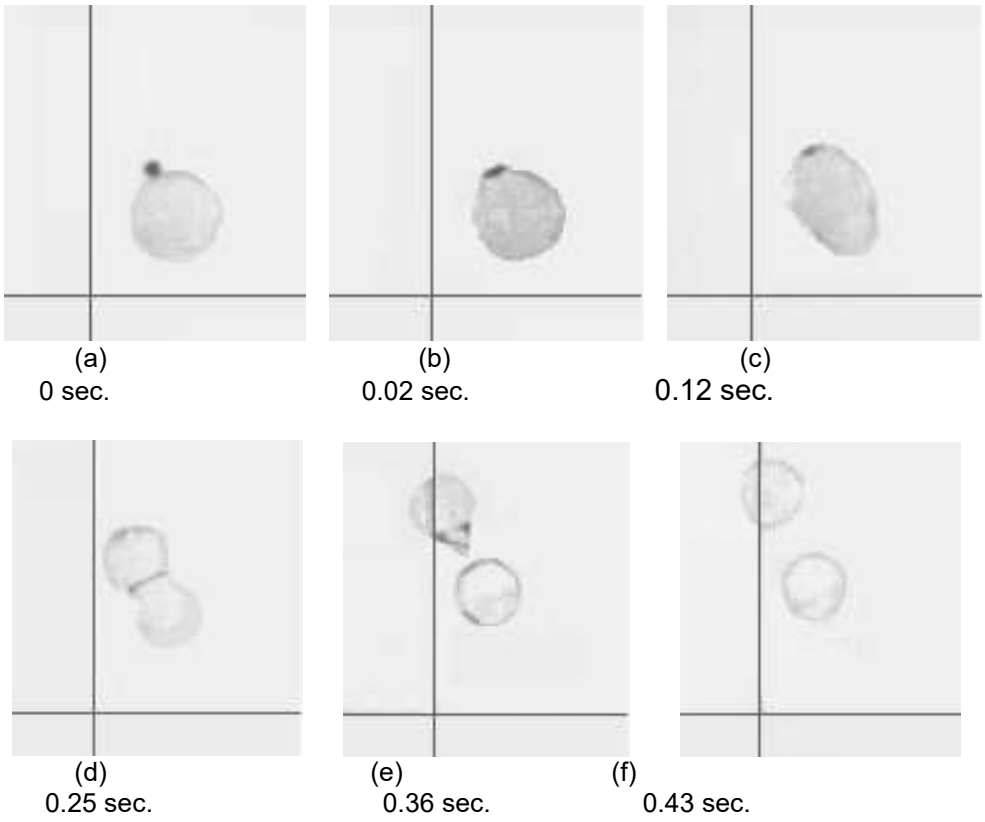

Fig. 7. Filmed pictures of the initial free drop (panel a), the deformed drop (b,c,d) and the break-up drop (e and f). The liquid/liquid (L/L') system is characterized by the system 3 given in Tables 1 and 2; $\Pi = 19.2$ dyn/cm; $\lambda = 0.94$; a = 0.46 cm; $F_M(0) = 28.57$ dyn.

Figure 7 illustrates the initial free drop (panel a), the drop deformations Figure 7(b, c, d), the drop movement (Figure 7d) and the break-up of the drop into two droplets (Figure 7e and f). This is the third case of a deformable drop observed for the system 3, and its detailed characterization is given in Tables 1 and 2. It can be seen that at a certain moment in time (Figure 7e) a tip in one of the drop compartments appears (Fig. 7e, upper droplet), and it might be an example of the tip-stretched effect.

As we can see, from Table 2, for system 1, the value of viscosities ratio, $\lambda >> 1$, is very large, and the value of the Marangoni force, $F_M(0)$, is slightly smaller than 1 dyn, and the drop is nondeformable (Figure 5). For systems 2 and 3, given in Table 2, the ratio values of the bulk viscosities are greater than unity, $\lambda > 1$ (system 2) or rather close to unity (system 3), and the Marangoni force, $F_M(0)$, is much higher than 1 (system 2) and the highest value is for system 3. Accordingly, system 2 represents a deformable free drop, shown in Figure 6, and system 3 signifies a deformable free drop for a short time followed by the break-up drop in two droplets, as given in Figure 7.

Figure 7 reveals the different shapes of the free drop dynamics. Because there is a variation of the drop shape, in this case, the surface dilution and capillary forces will appear. This is the situation of a slightly viscous drop, when the Marangoni effect will provoke the drop deformations, which will generate the surface dilution in parallel with the appearance of capillary forces (Figure 7b).

For the system 3, described in Tables 1 and 2, the viscosity of continuous bulk (μ) liquid and of the drop (μ') liquid are almost equal, $\lambda \approx 1$, Table 2, but the Marangoni force $F_M(0)$ takes the highest value (28.57 dyn). In this situation, after a few moments (at about 0.36 sec) the breakup of the drop appears (Figure 7e), and the drop is divided into two parts (droplets). This is the most complicated situation, when the Marangoni force will provoke the drop deformations, which will generate, in parallel, the surface dilution and the tip-stretching, until the drop is broken into two droplets, as illustrated in Figure 7 (e, f).

Under the surface tension gradients, the free drop movement lead to the appearance of the resultant Marangoni force, F_m, (Figure 3), with its normal F_n and tangential, F_t, components. In this investigation it is shown that the normal force component causes the drop deformations and it is the dominant force, for $\theta_f < \theta_0$, and it causes the hammer effect. The tangential force component provokes the displacement of the drop (such as lifting effect) and it is the major force for $\theta_f > \theta_0$.

At the moment of surfactant solution injection, the resultant Marangoni F_m force is negative, acting in the opposite direction of the normal to the drop surface. Small values of resultant Marangoni force F_m causes the visible modifications of the drop shape (Figure 6b,c). For $\theta_f > \theta_0$ the resultant force F_m becomes positive and its effect is the propulsion of the drop or the translational movement of the drop along the Oz

axis (Figure 6d,e). Big values of the resultant Marangoni force F_m causes the visible modifications of the drop shape (Figure 7b,c,d) and even the breakup of the drop (Figure 7e,f).

Marangoni flow is driven by a surface tension gradient, and it is crucial for the spreading of surfactants, such as fatty acids [33-36], lipids [37-40], proteins [41, 42], carotenoids mixed and lipids [43-46], as membrane models (e.g., Langmuir monolayers and Langmuir-Blodgett membranes) on a liquid interface (air/water, liquid/liquid or oil/water interfaces). By placing a surfactant at the air/water interface [44] or by its adsorption at the oil/water interface [47], a surface tension gradient appears, and the Marangoni flow spreads the surfactant across the interface.

In this context, the interfacial mechanism of anesthesia was explored by us, using procaine (a local anesthetic agent) and membrane models, like fatty acids [48,49] and phospholipids [50] monolayers, as well as human erythrocytes [51]. Clearly, this complex mechanism involves the Marangoni flow, where a fluid membrane interface is moved by a gradient of surface tension, caused by differences in the procaine concentration.

Additionally, anesthetic agent interacts with the erythrocyte membrane, altering its interfacial properties, as evidenced by atomic force microscopy [51]. The disruption of the initial interfacial equilibrium of erythrocyte membrane, by its interaction with anesthetic molecules, creates an interfacial tension gradient, generating a Marangoni flow within the red blood cell's surrounding fluid. This flow can facilitate the interfacial mechanism of anesthesia, as a result of the red blood cells' movement and their surrounding fluid movement.

.CONCLUSIONS

An advanced hydrodynamic model has been developed in which the interfacial tension gradients, caused by the addition of a surfactant or a surfactant solution on the well-defined free drop surface, will generate a Marangoni force primarily responsible for the drop deformations and movements. The drop deformation process is described and mathematically analyzed. It has been shown that it is a deep dependence of the absolute values of the Marangoni force $F_M(0)$ and the deformations of a free drop.

In other words, a small Marangoni force will not cause the deformations of the viscous drop, but a large Marangoni force will provoke complicated deformations and movements of a free drop even the breakup of the free drop. Thus, it is also shown experimentally and theoretically that the Marangoni force is a primary cause of the deformations of a free drop. Surface dilution and tip-stretching effects, as

well as the capillary forces, might appear as secondary factors in the drop deformation processes. The results of our theoretical hydrodynamic model are in substantial agreement with experimental observed data.

Certainly, it is to be emphasized that such complex interfacial phenomena, generated by Marangoni force and Marangoni instability, are a result of the adsorption of a surfactant at the surface between the two liquid phases. These phenomena are of a major interest, both in industrial and biological processes [48-51], in movements at the surface of biological membranes [52, 53], as well as in the space science and cosmos technology of liquids [1-7, 17, 25-32].

Moreover, the effects of surface tension on living cells [51-53] are crucial and might be explored in the new strategies for the treatment of various diseases, including nanostructured drug delivery systems [52] targeting the cancerous cells, with medical applications.

FUNDING: This research study was funded by a grant from the Ministry of Research, Innovation and Digitization, CNCS-UEFISCDI, project PN-III-P4-ID-PCE-2020-1910, project no. 186. We acknowledge the research support from the Ministry of Education and Research and Executive Agency for Higher Education, Research, Development and Innovation Funding in Romania for inter- and multi-disciplinary fundamental and exploratory research with cosmos applications for surface flow of liquids in the absence of gravity, as well for medical applications. This research work was performed at the Scientific Research Center of Excellence in Physical Chemistry, part of STAR Institute, Babes-Bolyai University. The founder (2006) and director (2006–present) of this Research Center is Maria Tomoaia-Cotisel.

ACKNOWLEDGMENT: We acknowledge the fruitful scientific research collaboration for *in vitro* and *in vivo* research studies carried out through this collaboration between Babes-Bolyai University, Research Center of Excellence in Physical Chemistry, and Iuliu Hatieganu University of Medicine and Pharmacy, Department of Orthopedics and Traumatology, by using the experimental facilities and top equipment for scientific research with medical applications.

REFERENCES

[1]. E. Chifu, "*Surface flow of liquids in the absence of gravity*", proposal selected by NASA's Office of Aeronautics and Space Technology, 1977, pp. 1-39.

[2]. E. Chifu and I. Stan**,** Rev. Roum. Chim. **25**, 1449 (1980).

[3]. E. Chifu, I. Stan**,** Z. Finta and E. Gavrila, J. Colloid Interface Sci. **93,** 140 (1983).

[4]. I. Stan, E. Chifu, Z. Finta and E. Gavrila, Rev. Roum. Chim. **34**, 603 (1989).

[5]. I. Stan**,** C.I. Gheorghiu and Z. Kasa, Studia Univ. Babes-Bolyai, Math. **38**(2), 113 (1993).

[6]. E. Chifu, I. Albu, C. I. Gheorghiu, E. Gavrila, M. Salajan and M. Tomoaia-Cotisel, Rev. Roum. Chim. **31**, 105 (1986).

[7]. I. Stan, E. Chifu and Z. Kasa, ZAMM, Z. angew. Math. Mech. **75**, 369 (1995).

[8]. R. S. Valentine, W. J. Heideger, Ind. Eng. Chem. Fund. **2**, 242 (1963).

[9]. R. S. Schechter, R. W. Farley, Canadian J. Chem. Eng. **41**,103 (1963).

[10]. M. D. Levan, J. Colloid Interface Sci. **83**, 11 (1981).

[11]. L. Landau and E. Lifschitz, *Mécanique des fluides,* (Ed. Mir, Moscou, 1971).

[12]. V. G. Levich, *Physicochemical Hydrodynamics*, Chap. VIII (Prentice-Hall, Englewood Cliffs, New Jersey, 1962).

[13]. T. Oroveanu, *Mecanica fluidelor vâscoase* (Ed. Acad., Bucharest, 1967).

[14]. L. E. Scriven, Chem. Eng. Sci. **12**, 98 (1960).

[15]. R. Aris, *Vectors, Tensors and the Basic Equations of Fluid Mechanics*, Chap. X. (Prentice-Hall, Englewood Cliffs, New Jersey, 1962).

[16]. A. Sanfeld, Physical Chemistry Series, (W. Jost, Ed.), Vol. I, (Acad. Press, New York, (1971).

[17]. I.R. Stan, M. Tomoaia-Cotisel, A. Stan, Romanian Reports in Physics. **61**(3), 451 (2009).

[18]. A. Wierschem, H. Linde and M. G. Velarde, Phys. Rev. E. **62,** 6522 (2000).

[19]. Y. T. Hu and A. Lips, Phys. Rev. Lett. **91**, 1 (2003).

[20]. H. A. Stone and L. G. Leal, J. Fluid Mech.*,* **220**, 161 (1990).

[21]. W. J. Milliken, H. A. Stone and L. G. Leal, Phys. Fluids, A. **5**, 69 (1993).

[22]. C. D. Eggleton and K. J. Stebe, J. Colloid Interface Sci. **208**, 68 (1998).

[23]. R. Savino, R. Monti, F. Nota, R. Fortezza, L. Carotenuto C. Picolo, Acta Astronautica **55**(3), 169 (2004).

[24]. G. K. Batchelor, *An Introduction to Fluid Mechanics* (Cambridge Univ. Press, Cambridge, 1967).

[25]. E. Chifu, I. Stan and M. Tomoaia-Cotisel, Rev. Roum. Chim. **50**, 297 (2005).

[26]. M.I. Salajan, A. Mocanu and M. Tomoaia-Cotisel, *Advances in Thermodynamics, Hydrodynamics and Biophysics of Thin Layers* (University Press, Cluj-Napoca, 2004).

[27]. I. R. Stan, M. Tomoaia-Cotisel, A. Stan, Bull. Transilvania Univ. Brasov, Series B1, Math. Informat. Phys. **13**(48), 357 (2006).

[28]. M. Tomoaia-Cotisel, E. Gavrila, I. Albu, I.-R. Stan, Studia, Univ. Babes-Bolyai, Chem. **52**(3), 7 (2007).

[29]. M. Tomoaia-Cotisel, A. Stan, I. R. Stan, Studia, Univ. Babes-Bolyai, Chem. **53**(4), 85 (2008).

[30]. I. R. Stan, M. Tomoaia-Cotisel, A. Stan, C. Borzan, Rev. Roum. Chim. **53**(6), 471 (2008).

[31]. I. R. Stan, M. Tomoaia-Cotisel, Analele Univ. Vest Timisoara, Seria Fizica. **50**, 86 (2007).

[32]. I. R. Stan, M. Tomoaia-Cotisel, A. Stan, PAMM - Proc. Appl. Math. Mech. **7**, 4100041-4100042 (2007); DOI 10.1002/pamm.200701036

[33]. M. Tomoaia-Cotisel, J. Zsako, A. Mocanu, M. Lupea and E. Chifu, J. Colloid Interface Sci. **117**(2), 464 (1987).

[34]. J. Zsako, M. Tomoaia-Cotisel, A. Mocanu and E. Chifu, J. Colloid Interface Sci. **110**(2), 317 (1986).

[35]. R. Katz, M. Tomoaia-Cotisel, M.C. Rattazzi and P. Fishman, J. Molec. Neurosci. **33**(1), 133 (2007).

[36]. J. Zsako, M. Tomoaia-Cotisel and E. Chifu, J. Colloid Interface Sci. **102**(1), 186 (1984).

[37]. M. Tomoaia-Cotisel, J. Zsako and E. Chifu, Ann. Chim. (Rome) **71**(3-4), 189 (1981).

[38]. M. Tomoaia-Cotisel, J. Zsako, E. Chifu and P.J. Quinn, Chem. Phys. Lipids **34**(1), 55 (1983).

[39]. M. Tomoaia-Cotisel, E. Chifu, J. Zsako, A. Mocanu, P.J. Quinn and M. Kates, Chem. Phys. Lipids **63**(1-2), 131 (1992).

[40]. M. Tomoaia-Cotisel and I.W. Levin, J. Phys. Chem. B **101**(42), 8477 (1997).

[41]. M. Tomoaia-Cotisel, A. Tomoaia-Cotisel, T. Yupsanis, G. Tomoaia, I. Balea, A. Mocanu, C. Racz, Rev. Roum. Chim. **51**(12), 1181 (2006).

[42]. I. Cojocaru, A. Tomoaia-Cotisel, A. Mocanu, T. Yupsanis, M. Tomoaia-Cotisel, Rev. Chim. (Bucharest) **68** (7), 1470 (2017).

[43]. M. Tomoaia-Cotisel and E. Chifu, J. Colloid Interface Sci. **95**(2), 355 (1983).

[44]. M. Tomoaia-Cotisel, J. Zsako, E. Chifu and D.A. Cadenhead, Langmuir **6**(1), 191 (1990).

[45]. M. Tomoaia-Cotisel, E. Chifu, J. Zsako, Colloids and Surfaces **14**(2), 239 (1985).

[46]. M. Tomoaia-Cotisel, J. Zsako, E. Chifu and P.J. Quinn, Biochem. J. **248**, 877 (1987).

[47]. P. Joos, A. Tomoaia-Cotisel, A.J. Sellers, M. Tomoaia-Cotisel, Colloids and Surfaces. B Biointerfaces **37**(3-4), 83 (2004).

[48]. M. Tomoaia-Cotisel, Progr. Colloid. Polym. Sci. **83**, 155 (1990).

[49]. J. Zsako, M. Tomoaia-Cotisel, E. Chifu, A. Mocanu and P.T. Frangopol, Biochim. Biophys. Acta (BBA)-Biomembranes **1024**(2), 227 (1990).

[50]. A. Mocanu, P. J. Quinn, C. Nicula, S. Riga, G. Tomoaia, C.-A. Bardas, M. Tomoaia-Cotisel, Rev. Roum. Chim., **66**(10-11), 855 (2021).

[51]. U.V. Zdrenghea, G. Tomoaia, D.V. Pop-Toader, A. Mocanu, O. Horovitz, M. Tomoaia-Cotisel, Comb. Chem. High Throughput Screen. **14**(4), 237 (2011).

[52]. A. Mocanu, M.A. Ujica, O. Horovitz, G. Tomoaia, O. Soritau, C.T. Dobrota, C.R. Popa, A. Kun, H.R.C. Benea, I.M. Mang, G. Borodi, V. Raischi, M. Roman, L.C. Pop, M. Tomoaia-Cotisel, *Biomedicines*. **13**(8), 1861 (2025).

[53]. M.A. Ujica, C.T. Dobrota, G. Tomoaia, C.L. Roșoiu, A. Mocanu, M. Tomoaia-Cotisel, Annals Series on Biological Sciences. **14**(1), 139 (2025).